Distribuição de tensões ao redor de implantes com pilares protéticos de diferentes materiais: comparação entre análise fotoelástica, extensometria e elementos finitos

Article *in* Revista Odonto Ciencia · March 2016

DOI: 10.15448/1980-6523.2015.4.14816

CITATIONS
0

READS
116

6 authors, including:

Mayra Cardoso
Universidade Veiga de Almeida (UVA)
22 PUBLICATIONS **103** CITATIONS
SEE PROFILE

Pedro Henrique Corazza
Universidade de Passo Fundo
40 PUBLICATIONS **470** CITATIONS
SEE PROFILE

Alexandre Luiz Souto Borges
São Paulo State University
192 PUBLICATIONS **836** CITATIONS
SEE PROFILE

Marco Antonio Bottino
São Paulo State University
458 PUBLICATIONS **5,770** CITATIONS
SEE PROFILE

Revista Odonto Ciência
Journal of Dental Science

ORIGINAL ARTICLE

Rev Odonto Cienc 2015;30(4):132-137
http://revistaseletronicas.pucrs.br/ojs/index.php/fo
http://dx.doi.org/10.15448/1980-6523.2015.4.14816

Open Access

Stress distribution around implants with abutments of different materials: a comparison of photoelastic, strain gage and finite element analyses

Mayra Cardoso[a], Pedro Henrique Corazza[a], Cristiane Aparecida de Assis Claro[b], Alexandre Luiz Souto Borges[a], Marco Antonio Bottino[a], Lafayette Nogueira Junior[a]

Abstract

Objective: To compare stress transmission around implants with abutments made of three different materials using photoelastic, strain gage (SGA) and finite element (FEA) analyses.

Methods: Three abutments – UCLA calcinable, cast in Ni-Cr; UCLA calcinable with a Cr-Co cervical collar, overcast with Ni-Cr; and a zirconia abutment – were installed on implants embedded in photoelastic resin. Vertical and oblique loads were applied to the abutments to the photoelastic and SGA analyses. Data were analyzed by Kruskal-Wallis and Mann-Whitney tests (a=0.05). The assembly was modeled to FEA simulation.

Results: Similar fringe orders were observed in the apical region under vertical load. The greatest fringe orders were observed in the coronal region of the opposite side of load application (contralateral side) under oblique load. By SGA, no statistical difference was observed among the abutments (P=0.061) under vertical load, and no difference was found between tensile and compression sides under oblique load. FEA showed no difference in stress distribution. The oblique load generated the greatest stress values on the contralateral side in the coronal area.

Conclusion: Although it was not possible to establish an agreement among the analytical methods tested, different abutment materials did not influence the transmission of stresses around implants.

Key words: Abutment design; Bite force; Dental implants; Stress analysis: Tension

[a] Unesp – Univ Estadual Paulista, São José dos Campos, SP, Brazil
[b] University of Taubaté, Taubaté, SP, Brazil

Distribuição de tensões ao redor de implantes com pilares protéticos de diferentes materiais: comparação entre análise fotoelástica, extensometria e elementos finitos

Resumo

Objetivo: Comparar a transmissão de tensões ao redor de implantes com pilares protéticos de três materiais diferentes, por meio de análise fotoelástica, extensometria e elementos finitos.

Métodos: Três pilares protéticos – UCLA calcinável fundido em Ni-Cr, UCLA calcinável com colar cervical em Cr-Co sobrefundido em Ni-Cr, e pilar de zircônia – foram instalados sobre implantes embebidos em resina fotoelástica. Aplicou-se carga vertical e oblíqua sobre os pilares para a análise fotoelástica e a extensometria. Os dados foram analisados pelo teste de Kruskal-Wallis e Mann-Whitney (a=0,05). O conjunto foi modelado para simulação com elementos finitos.

Resultados: Ordens de franja semelhantes foram observadas na região apical sob carga vertical. As maiores ordens de franja foram observadas na região coronal do lado oposto à aplicação da carga oblíqua. Por extensometria, não foi observada diferença estatisticamente significante entre os pilares (P=0,061) sob carga vertical, e não foi observada diferença entre os lados de tração e compressão sob carga oblíqua. A análise por elementos finitos não mostrou diferença na distribuição de tensões. A carga oblíqua gerou os maiores valores de tensão no lado oposto na região coronal.

Conclusão: Embora não tenha sido possível estabelecer uma concordância entre os métodos testados, diferentes materiais do pilar protético não influenciaram a transmissão de tensões ao redor de implantes.

Palavras-chave: Desenho do pilar protético; Força de mordida; Implantes dentários; Análise de tensões

Correspondence:
Mayra Cardoso
mayracardoso.mc@gmail.com

Received: October 26, 2013
Accepted: December 1, 2015

Conflict of Interests: The authors state that there are no financial and personal conflicts of interest that could have inappropriately influenced their work.

Introduction

Masticatory functional loads are normally transferred through the implants to the peri-implant bone [1]. Bone can tolerate physiologic loads, but excessive stresses may result in resorption, leading to esthetic cervical defects and implant loss [2]. Stress distribution around implants depends on several factors, such as implant design and diameter [3], abutment length [4], angulation [1] and its relationship with the implant platform [5]. However, the influence of abutment material or manufacturing processes has not been properly investigated. It is known that the abutment material influences the location and quality of the peri-implant mucosa attachment [6], but differences in physical properties of abutments, such as elastic modulus or marginal fit could play a role in stress distribution in bone. De Torres et al. [7] reported that framework material influence bone stress, although Abreu et al. [8] did not find this correlation.

Among the methods to analyze the transmission of stresses to bone, the most common are photoelastic, strain gage and finite element analyses. Photoelastic analysis is a low cost simple method, and provides a qualitative overview of the stresses formed in the bone tissue but does not allow an accurate measure [9]. Strain gauges measure the deformation of a body by measuring the change in its electrical resistance. They provide quantitative data and can be used *in vivo*. However, their size and placement are critical, and can be limiting factors [9]. Several studies have found good correlation between the two methods [3,10], however, one study showed different results between them [1].

The finite element analysis is a quite versatile numerical method that allows distinguishing materials by their physical properties, such as internal architecture and modulus of elasticity [11]. Several studies have compared this method with strain gauge analysis, and the results are controversial. Eser et al. [12] studied the biomechanics of implant overdentures *ex vivo* and found a high degree of consistency between the two methods in detecting bone deformities, both qualitatively and quantitatively. Other researches also suggest a good correlation between them [13,14]. Iplikcioglu et al. [15] found compatibility between the methods when analyzing a cone-morse implant system under vertical force, but not under oblique force. In another study by Akça et al. [16] there was agreement on the quality of the deformation induced, however, the quantification of this deformation differed between the methods.

The compatibility of stress distribution assessment methods is still controversial in dental literature. Thus, the objectives of the present study were [1] to compare the transmission of stresses around implants with prosthetic abutments made of different materials using photoelastic, strain gage and finite element analyses; and [2] to compare the three experimental methods.

Methods

Fabrication of test models and photoelastic analysis

Three abutments (Conexão Sistema de Próteses – São Paulo, Brazil) were used in this study: a UCLA calcinable abutment, which was cast in Ni-Cr (called Ni-Cr abutment); a UCLA calcinable abutment with a Cr-Co cervical collar, which was overcast with Ni-Cr (called Ni-Cr/Cr-Co abutment); and a zirconia abutment. The abutments were veneered with a layer of feldspathic ceramic, resulting in an approximated final dimension of 11.0 mm in high and 5.0 mm in diameter. The abutments were retained by titanium screws on three external hexagon implants (Conexão Sistema de Próteses), 13×3.75 mm with a 4.1 mm diameter platform, with a 20 Ncm torque.

Each implant/abutment assembly was placed precisely into a socket prepared on the top of a polyamide block (3×4×1.5 cm), positioning the collar according to the manufacturer's recommendations. An impression was made of the entire set (Silibor, Artigos Odontológicos Clássico – São Paulo, Brazil), and after the impression material had set, the polyamide block was removed and photoelastic resin (Araldite GY 279 BR, Araltec Produtos Químicos Ltda. – Guarulhos, Brazil) was poured into the mold. After 24 h, the photoelastic resin models were removed and polished.

Each model was placed in the field of a circular polariscope and inspected to ensure its stress-free condition (maximum of 0.45 fringe order). A static load of 147 N (vertical and oblique) was applied on the abutment and the isochromatc fringes were photographed by a digital camera. For oblique load application, the models were positioned on a plane inclined at 25-degrees.

Strain gauge analysis

Two strain gauges (PA-06-062AB-120-L, Excel Sensores – Embú, Brazil) were bonded onto the surface of each photoelastic resin block on both sides of the implant. The distance from the gauge grid to the implant was standardized at 1 mm.

The gauges were connected to a data acquisition machine (ADS 2000, Lynx Tecnologia Eletrônica Ltda. – São Paulo, Brazil). Load application followed the same protocol previously described. Strain gauge signals were collected for 10 s (500 readings per channel), and were digitized, amplified and analyzed by the software AqDados (Lynx Tecnologia Eletrônica Ltda.). The magnitude of deformation in each gauge was recorded in micro-deformations (με). Before each measurement, the apparatus was reset to zero, balanced and calibrated to ±10 με. Five measurements were obtained for each model, and the lowest and the highest were discarded. For oblique load application, the values of the two gauges were considered separately. For vertical load application, we considered the mean values from the two gauges together. Data were compared by Kruskal-Wallis analysis of variance at a 95% confidence level for each vertical load, compression and tensile sides of oblique load. Mann-Whitney's test was

applied to compare compression and tensile sides for each abutment.

Finite element analysis

Digital radiographs of an implant and an abutment were taken as a basis for designing the models, which were created according to the implant and abutment shapes in a modeling program (Rhinoceros 4.0 – Seattle, USA). The models were exported to a simulation program (Ansys – Canonsburg, USA) where the material properties were inserted according to Table 1.

Table 1. Elastic modulus (E) and Poisson's ratio (v) of the materials used in FEA analysis

Material	E (GPa)	v
Yttria-stabilized zirconia ceramic (22)	209.3	0.32
Feldspathic ceramic (22)	66.5	0.21
Comercially pure titanium (23)	110	0.35
Ni-Cr alloy (24)	188	0.33
Cr-Co alloy (25)	218	0.33
Photoelastic resin	2.07	0.41

The FEA simulations were developed with two types of abutment (zirconia abutment and Ni-Cr abutment), in which the difference between them was dictated by the elastic modulus. It was assumed that all solids were homogeneous, isotropic and linear elastic. As the aim of the study was to analyze the stress distribution in the photoelastic resin only, and not on the abutment/implant joint, the components were considered perfectly bonded, and there were no flaws in the components. A mesh of 69817 elements and 118637 nodes was created after the convergence test. The convergence was performed changing the size of elements to reach less than 10% of variation. The contact region between the implant and the basis (0.5 mm minimum size) was refined. The support base was fixed in three axes, and the stress was generated from vertical and oblique loads, both of 147 N. The vertical load was applied vertically on the top of the abutment. The 147 N total load was decomposed into two vectors (x=62.12 N; y=133.23 N) to result in the 25-degree oblique load. The comparison between the abutment types was performed by Von Mises analyses of the photoelastic resin basis.

Results

Photoelastic analysis

Figure 1 presents the isochromatic fringe patterns of the three abutments under vertical and oblique load. Fringe orders are presented in Table 2. Under vertical load, the fringe orders in the apical region of zirconia abutment were the same as those in the Ni-Cr abutment, and slightly greater than those in the Ni-Cr/Cr-Co abutment. In the coronal region, the fringes were not clear and were disregarded. Under oblique load, the greatest fringe orders were observed in the coronal region of the compression side (contralateral side). In this region, Ni-Cr and Ni-Cr/Cr-Co abutments showed the same fringe orders, slightly higher than those of the zirconia abutment. In the apical region, stresses were greater on the compression side (loaded side), being greater with zirconia abutment, followed by the Ni-Cr and Ni-Cr/Cr-Co abutments.

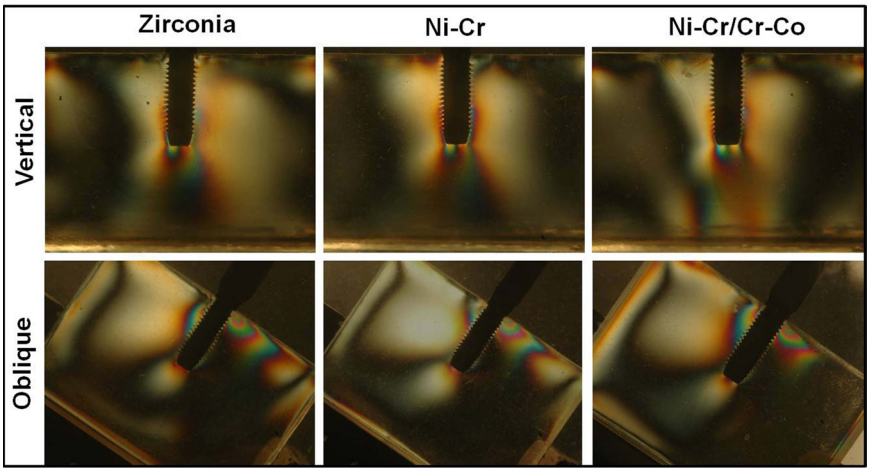

Figure 1. Isochromatic fringe patterns of the three abutments under vertical and oblique load.

Table 2. Isochromatic fringe orders around implants

Abutment	Vertical load		Oblique load Loaded side		Oblique load Contralateral side	
	Apical	Coronal	Apical	Coronal	Apical	Coronal
Zirconia	1.81	–	1.06	1.38	0.90	3.60
Ni-Cr	1.81	–	1.00	0.60	0.90	4.00
Ni-Cr/Cr-Co	1.38	–	0.60	2.50	0.60	4.00

Strain gauge analysis

Comparison of the results provided by strain gauge analysis for each type of abutment is shown in Table 3. The values resulting from the vertical load did not differ statistically irrespective of the abutment material (P=0.061). When an oblique load was applied to the models, there was no statistical difference among the abutments for both compression side (P=0.061) or tensile side (P=0.058). Mann-Whitney's test revealed no difference between tensile and compression sides when an oblique force was applied to zirconia (P=0.820), Ni-Cr (P=0.662) or Ni-Cr/Cr-Co abutments (P=1.000).

Table 3. Median (Interquartile Range) of microstrain around implants in the coronal region ($\mu\varepsilon$)

Abutment	Vertical load	Oblique load Compression side	Oblique load Tensile side
Zirconia	5.99 (4.84)	5.10 (2.14)	5.92 (3.48)
Ni-Cr	1.51 (0.24)	2.71 (3.53)	3.57 (2.59)
Ni-Cr/Cr-Co	3.54 (1.09)	10.27 (1.85)	10.01 (6.10)

Finite element analysis

Von Mises analysis of the two types of abutments showed no difference in the stress distribution, both with vertical and oblique load (Figure 2). The vertical load resulted in a symmetric stress pattern with the greatest concentration around the coronal portion (6.81 MPa) and apical end (4.38 MPa). The oblique load generated the highest stress values on the contralateral side in the coronal area (20.35 MPa). In the coronal area on the loaded side, the highest stresses recorded were 14.25 MPa. In the apical regions, the highest stresses were 4.07 MPa on the loaded side and 6.1 MPa on the contralateral side.

Discussion

The improvement in mechanical properties of ceramic materials has enabled their use as prosthetic abutments, especially zirconia, which combines strength and esthetic properties [17]. However, it is not clear if the transmission of masticatory loads to the bone around implants is similar between zirconia and conventional metal abutments. The results of the present study suggest that the stress distribution in bone is independent of abutment material.

In general, both photoelastic and finite element analysis showed that when an oblique load is applied to an implant, the stresses concentrate mainly in the coronal region of the contralateral side, followed by the apical region of the loaded side; these two regions are compressive areas. These results show a qualitative correlation between the two analytical methods, although a quantitative correlation cannot be assumed. These findings are in agreement with the results of Ozcelik & Ersoy [18], who studied stresses in tooth-implant prostheses, and de Vree et al. [19], who compared the two methods in tooth structures.

The strain gauge analysis failed to show the difference between the two sides in the coronal region with oblique load application, possibly due to a high coefficient of variation, inherent to the test, or to the unidirectional position of the gauges. According to Karl et al. (9), different forces may lead to similar readings of unidirectional strain gauges. Moreover, the measuring grids of the gauges were not

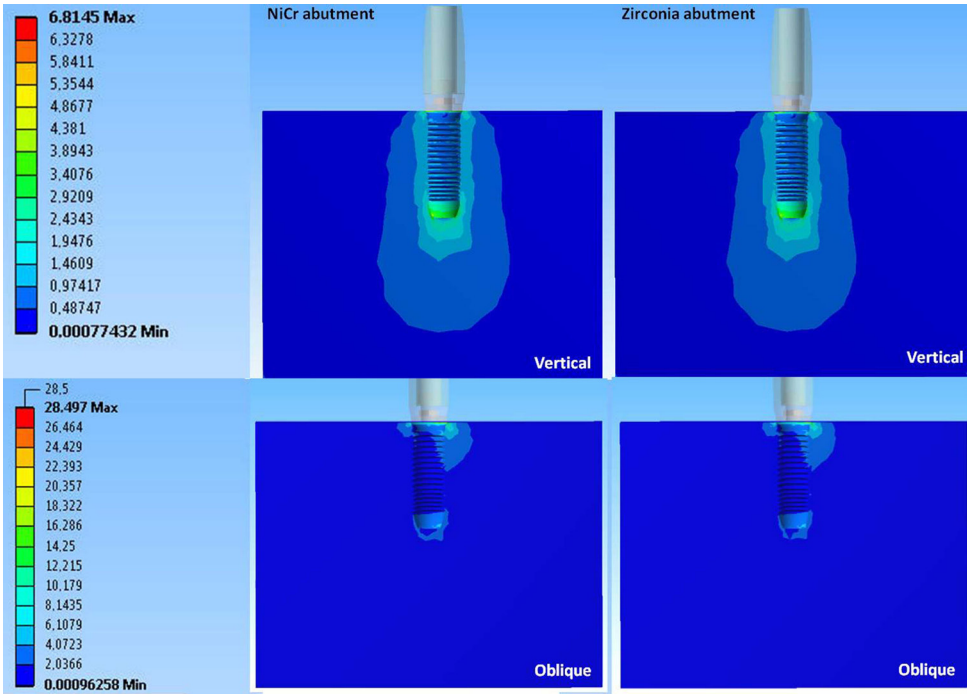

Figure 2. Von Misses analysis comparing NiCr and zirconia abutments after vertical and oblique loads.

allowed to touch the implant collar, where higher stresses are observed, because of the polyamide backing of the gauges. However, cutting away this backing would diminish the gauge sensitivity [20].

Under vertical load, both strain gauge and finite element analysis revealed no differences among the abutments. Only under this load condition can agreement between the two methods be assumed, as previously demonstrated by Iplikcioglu et al. [15]. For the photoelastic analysis, the fringes were not clear enough to enable a comparison in the coronal region, and for this reason, the area was excluded from the analyses, precluding a comparison between photoelastic and strain gauge analysis. The applied force may not have been sufficient to produce a clear fringe pattern in this area, since other photoelastic studies have shown little stress in this area and stress concentration at the apical end of the implant [1,3]. In this regard, the present study is in agreement with previous studies. In the apical region, the Ni-Cr/Cr-Co abutment showed the less stress concentration, but the difference was only two colors within the same fringe order.

The stress distribution observed in the finite element analysis showed no difference between the Ni-Cr and the zirconia abutments models. Due to these results, the third model (Ni-Cr/Cr-Co abutment model) was not simulated, since the relative difference in elastic modulus between zirconia and Cr-Co is smaller than the difference between zirconia and Ni-Cr, and the volume of Cr-Co alloy in Ni-Cr/Cr-Co abutment is small in comparison with that contained in the whole abutment.

This study hypothesized that a difference in abutment material could influence stress distribution in peri-implant bone, due to differences in elastic modulus or marginal fit. This hypothesis was not confirmed. De Torres et al. [7] found that Cr-Co alloy frameworks transmitted more stress to the implants than commercially pure titanium and Ni-Cr-Ti alloy. They attributed these results to the difference in the elastic modulus of the materials. Nevertheless, their study assessed frameworks over five implants, whereas the present study assessed abutments over individual implants. As calcinable abutments tend to produce greater misfits than machined ones [21], it was supposed that this could also influence stress transmission to bone. Although misfit was not assessed in this study, it is reasonable to assume that misfit was greater at the Ni-Cr abutment than at the Ni-Cr/Cr-Co abutment. The similarity of stress transmission between these abutments corroborates the results of previous studies that found no correlation between prosthesis-implant misfit and stress transmission [7,8].

This study could not establish an agreement among the three analytical methods tested. There was a difference in the stress distribution pattern between photoelastic and finite element analysis with vertical load, although there were qualitative similarities with oblique load. Photoelastic analysis was the only method to show differences among the abutments, but these differences were small, often less than one fringe order. These findings suggest that they should be considered as complementary methods.

Conclusions

Within the limitations of this *in vitro* study, it could be concluded that:

1. Different abutment materials did not influence the transmission of stresses around implants;
2. It was not possible to establish an agreement among the analytical methods tested; when correlation occurred, it was only qualitative and dependent on loading condition.

Acknowledgements

The authors thank Conexão Sistema de Próteses (São Paulo, Brazil) for providing the implants and implant components.

References

1. Brosh T, Pilo R, Sudai D. The influence of abutment angulation on strains and stresses along the implant/bone interface: comparison between two experimental techniques. J Prosthet Dent 1998;79:328-34.
2. Chun HJ, Shin HS, Han CH, Lee SH. Influence of implant abutment type on stress distribution in bone under various loading conditions using finite element analysis. Int J Oral Maxillofac Implants 2006;21:195-202.
3. Akça K, Cehreli MC. A photoelastic and strain-gauge analysis of interface force transmission of internal-cone implants. Int J Periodontics Restorative Dent 2008;28:391-9.
4. Rubo JH, Souza EA. Finite element analysis of stress in bone adjacent to dental implants. J Oral Implantol 2008;34:248-55.
5. Rossi F, Zavanelli AC, Zavanelli RA. Photoelastic Comparison of Single Tooth Implant-abutment Bone of Platform Switching vs Conventional Implant Designs. J Contemp Dent Pract 2011;12:124-30.
6. Linkevicius T, Apse P. Influence of abutment material on stability of peri-implant tissues: a systematic review. Int J Oral Maxillofac Implants 2008;23:449-56.
7. de Torres EM, Barbosa GA, Bernardes SR, de Mattos Mda G, Ribeiro RF. Correlation between vertical misfits and stresses transmitted to implants from metal frameworks. J Biomech 2011;44:1735-9.
8. Abreu RT, Spazzin AO, Noritomi PY, Consani RL, Mesquita MF. Influence of material of overdenture-retaining bar with vertical misfit on three-dimensional stress distribution. J Prosthodont 2010;19:425-31.
9. Karl M, Dickinson A, Holst S, Holst A. Biomechanical methods applied in dentistry: a comparative overview of photoelastic examinations, strain gauge measurements, finite element analysis and three-dimensional deformation analysis. Eur J Prosthodont Restor Dent 2009;17:50-7.
10. Clelland NL, Gilat A, McGlumphy EA, Brantley WA. A photoelastic and strain gauge analysis of angled abutments for an implant system. Int J Oral Maxillofac Implants 1993;8:541-8.
11. Mellal A, Wiskott HW, Botsis J, Scherrer SS, Belser UC. Stimulating effect of implant loading on surrounding bone. Comparison of three numerical models and validation by in vivo data. Clin Oral Implants Res 2004;15:239-48.
12. Eser A, Akça K, Eckert S, Cehreli MC. Nonlinear finite element analysis versus ex vivo strain gauge measurements on immediately loaded implants. Int J Oral Maxillofac Implants 2009;24:439-46.
13. Baiamonte T, Abbate MF, Pizzarello F, Lozada J, James R. The experimental verification of the efficacy of finite element modeling to dental implant systems. J Oral Implantol 1996;22:104-10.
14. Palamara JE, Palamara D, Messer HH. Strains in the marginal ridge during occlusal loading. Aust Dent J 2002;47:218-22.
15. Iplikcioglu H, Akça K, Cehreli MC, Sahin S. Comparison of non-linear finite element stress analysis with in vitro strain gauge measurements on a Morse taper implant. Int J Oral Maxillofac Implants 2003;18:258-65.
16. Akça K, Cehreli MC, Iplikcioglu H. A comparison of three-dimensional finite element stress analysis with in vitro strain gauge measurements on dental implants. Int J Prosthodont 2002;15:115-21.
17. Yuzugullu B, Avci M. The implant-abutment interface of alumina and zirconia abutments. Clin Implant Dent Relat Res 2008;10:113-21.
18. Ozcelik T, Ersoy AE. An investigation of tooth/implant-supported fixed prosthesis designs with two different stress analysis methods: an *in vitro* study. J Prosthodont 2007;16:107-16.

19. de Vree JH, Peters MC, Plasschaert AJ. A comparison of photoelastic and finite element stress analysis in restored tooth structures. J Oral Rehabil 1983;10:505-17.
20. Cehreli M, Duyck J, De Cooman M, Puers R, Naert I. Implant design and interface force transfer. A photoelastic and strain-gauge analysis. Clin Oral Implants Res 2004;15:249-57.
21. Bondan JL, Oshima HM, Segundo RM, Shinkai RS, Mota EG, Meyer KR. Marginal fit analysis of premachined and castable UCLA abutments. Acta Odontol Latinoam 2009;22:139-42.
22. Borba M, de Araújo MD, de Lima E, Yoshimura HN, Cesar PF, Griggs JA, et al. Flexural strength and failure modes of layered ceramic structures. Dent Mater 2011;27:1259-66.
23. Turcio KH, Goiato MC, Gennari Filho H, dos Santos DM. Photoelastic analysis of stress distribution in oral rehabilitation. J Craniofac Surg 2009;20:471-4.
24. Morris HF. Veterans Administration Cooperative Studies Project No. 147/242. Part VII: The mechanical properties of metal ceramic alloys as cast and after simulated porcelain firing. J Prosthet Dent 1989;61:160-9.
25. Rubo JH, Capello Souza EA. Finite-element analysis of stress on dental implant prosthesis. Clin Implant Dent Relat Res 2010;12:105-13.